Saudi Journal of Biological Sciences 27 (2020) 2221–2226

Contents lists available at ScienceDirect

Saudi Journal of Biological Sciences

journal homepage: www.sciencedirect.com

Original article

Al (III) metal augment thermal aggregation and fibrillation in protein: Role of metal toxicity in neurological diseases

Mohd Shahnawaz Khan [a,*], Shams Tabrez [b], Md Tabish Rehman [c], Majed S. Alokail [a]

[a] Protein Research Chair, Department of Biochemistry, College of Sciences, King, Saud University, Riyadh, Saudi Arabia
[b] King Fahd Medical Research Center, King Abdulaziz University, Jeddah, Saudi Arabia
[c] Department of Pharmacognosy, College of Pharmacy, King Saud University, Riyadh, Saudi Arabia

ARTICLE INFO

Article history:
Received 2 February 2020
Revised 17 April 2020
Accepted 3 May 2020
Available online 11 May 2020

Keywords:
Fibrillar aggregates
Metal ion toxicity
Neurodegeneration
Serum albumin

ABSTRACT

Protein fibrillation is a leading cause of innumerable neurodegenerative diseases. The exact underlying mechanism associated with the formation of fibrils is yet to be known. Recently, the role of metal ions resulting into fibrillation of proteins has gained attention of the scientific community. In this piece of work, we have investigated the effect of the aluminum (Al) metal ion on the kinetics of aggregation of bovine serum albumin (BSA) protein under physiological conditions by employing several biophysical and microscopic techniques. Quenching of tryptophan fluorescence was observed along with 9 nm blue shift, demonstrating BSA becomes more hydrophobic during unfolding pathway of thermal denaturation. Moreover, ANS (8-Anilino-1-naphthalene sulfonic acid) binding shows quenching in fluorescence intensity with increasing time of incubation at 65 °C, suggesting unfolding leading to the disruption of hydrophobic patches in BSA. Besides, Thioflavin T intensity indicated a significant acceleration in BSA fibrillation at a ratio of 1:1 and 1:2 of BSA and Al (III) metal ion respectively. In addition, circular dichroism (CD) spectroscopy study revealed the transition of BSA from α-helical conformation to the β-sheet rich structure. Molecular docking analysis demonstrated significant binding affinity (−1.2 kcal/mol) of Al (III) with BSA involving Phe501, Phe506, Val575, Thr578, Gln579, Leu531 residues. Transmission electron microscopy (TEM) reaffirm augmentation of thermal-induced BSA fibril formation in the presence of Al (III) metal ions. This study highlights the metal chelating potency as the possible therapeutic target for neurological diseases.

1. Introduction

Proteins are the most fascinating class of biological macromolecules that play a major role in almost every stage of life. To perform proper function, the protein must be folded into compact globular structure and improper folding could lead to the degradation of protein by ubiquitination. The protein quality check machinery is quite efficient in removing these misfolded proteins. However, some of them escape this quality check and left out as a misfolded protein. These proteins act as a seed to fibrils, aggregate, and inclusion bodies, leading to various pathological conditions. There are myriad of neurodegenerative diseases which results due to the fibrillation, and aggregation of their essential proteins like α-synuclein, tau, amyloid-β etc. (Obrenovich et al., 2020; Vaquer-Alicea & Diamond, 2019; Taylor et al., 2002; Sacchettini & Kelly, 2002).

Protein aggregation is suggested to be connected with environmental factors, amongst which, imbalance in metal ion homeostasis is one of the significant factor (Huang et al., 2019; Mezzaroba et al., 2019; Xu et al., 2016). There are many scientific documents that advocate the presence of metal ions in the amyloid plaques of Alzheimer's disease, Lewy's bodies of Parkinson's disease, and in other amyloidosis markers (Islam et al., 2019; Jabir et al., 2018; Khan et al., 2012). Moreover, fibrillation is the process where a polypeptide travels from its native conformation to fibrillar aggregates, which are predominantly cross-beta sheets rich and can easily escape to the cellular degradation process (Mitra, 2019; Khan et al., 2016).

* Corresponding author.
E-mail address: moskhan@ksu.edu.sa (M. Shahnawaz Khan).
Peer review under responsibility of King Saud University.

Production and hosting by Elsevier

https://doi.org/10.1016/j.sjbs.2020.05.013
1319-562X/

Aluminum (Al) is the 3rd most abundant element in the earth's crust. It is also commonly found in contaminated drinking water and processed foods. Its oxide is frequently utilized as an effective adjuvant in vaccines to promote immune activation. A significant concentration of Al (nearly 300–600 mg/tablet) is also present in various medicines such as antiperspirants, buffered aspirin, and antacids (Bondy, 2016).

Aluminum enters the vascular system of the human through processed food and drinking water through the gastrointestinal tract (Priest et al., 1998). In the serum, most of the metal ions and salts are mainly bound to transferrin protein and serum albumin (Ott et al., 2019; Mishra et al., 2019; Hedberg et al., 2015). The serum metal ions could be transported to the nervous system by crossing the blood–brain barrier through receptor-mediated endocytosis of transferrin. The aluminum-protein complexes of around 0.005% can enter the brain by receptor-mediated endocytosis ultimately resulting into excess inflammatory activity within the brain (Maczurek et al., 2008; Yokel et al., 2001). The inflammations without any infectious agent (virus or bacteria) switch on the alarming condition of the immune system and promote stresses to brain cells leading to several neurodegenerative diseases. In addition, the deposition of aluminum ions in the nervous system causes inflammation which contributes to a rapid burst of reactive oxygen species (ROS). The produced ROS augments fragmentation of residential protein and conformational deterioration leading to damages to brain cells and pathological conditions (Agnihotri & Kesari, 2019; Huat et al., 2019).

There is a consistent body of information that reinforces the likelihood of aluminum as an agent that promotes brain aging (Bondy, 2014). Therefore, we investigated the effect of Al (III) on the kinetics of thermal-induced conformational changes in BSA as model protein and its fibrillation. The characterization of protein fibrillation/aggregation was done using various techniques like fluorescence, circular dichroism, and transmission electron microscopy.

2. Materials and methods

2.1. Materials

BSA, ANS, and Thioflavin T (ThT), were purchased from Sigma Chemicals Co. (St. Louis, MO, USA). $AlCl_3$ and other chemicals used in this study were of high analytical grade.

2.2. Methods

2.2.1. Preparation of fibril

BSA was dissolved in 20 mM sodium phosphate buffer (pH 7.4), and the concentration was measured spectrophotometrically at 280 nm using a molar extinction coefficient of 6.5 $M^{-1}.cm^{-1}$ (Nusrat et al., 2016). Aliquots for fibril preparation were prepared using a fixed concentration of BSA (150 μM) and heated at 65 °C for 5 h. In case of Al (III) sets, the BSA to Al (III) ratio was kept as 1:1 and 1:2. Aliquots were taken after every 1 h for performing spectroscopic assays. To avoid any inaccuracy, three replicates of each set were analysed. Stock of $AlCl_3$ (1 M) was prepared in double distilled water. Two different concentration of $AlCl_3$, 150 and 300 μM were used in our study.

2.2.2. Intrinsic fluorescence: Conformational measurement

Tryptophan specific fluorescence of native and denatured BSA was measured on a spectrofluorophotometer (Jasco FP-750, Japan) in a 10 mm path length quartz cell. The wavelength of excitation was kept at 295 nm and emission spectra were recorded between 310 and 400 nm. The concentration of BSA was kept 4 μM.

2.2.3. Extrinsic fluorescence assay: Hydrophobicity analysis

ANS (8-Anilino-1-naphthalene sulfonic acid) dye was employed to investigate the hydrophobicity of thermal denatured BSA (Ahmed et al., 2017). ANS dye was used 50 times higher concentration than BSA (4 μM) and the samples were incubated for 30 min in the dark before analysis. Emission spectra were recorded between 400 and 600 nm after excitation at 380 nm.

2.2.4. Far UV-CD spectroscopy

Far UV-CD spectra were measured on applied photophysics Chirascan spectrophotometer using a quartz cuvette of 1 mm path length. BSA under thermal stress (65 °C) was aliquoted at different point of time (1–5 h) and scanned between 190 and 250 nm wavelengths. BSA was diluted to 0.2 mg/ml with 20 mM sodium phosphate buffer pH 7.4 before analysis. The scanning was done at a rate of 100 nm/min with the response time of 1 s.

2.2.5. Kinetics of aggregation: Thioflavin T assay

An increase in ThT fluorescence intensity is widely used for the detection of amyloid formation (Khan et al., 2020; Xue et al., 2017). The kinetics of fibrillation of thermal denaturating BSA and in the presence of Al (III) were measured using ThT fluorescence assay (Biancalana & Koide, 2010). Aliquot samples (4 μM) was mixed with 8 μM of ThT and incubated for 30 min in the dark before spectral measurement. The emission spectra were recorded between 450 and 550 nm after excitation at 440 nm. The path length of quartz cuvette was 1 cm.

2.2.6. Transmission electron microscopy (TEM) analysis

10 μL of all incubated samples (BSA control, denatured BSA & BSA-Al complex) were placed on Formvar carbon-coated copper grids for 10 min and air-dried at room temperature. These samples were further stained with 2% uranyl acetate for 5 min and photographed on a TEM system (JEOL Inc., Tokyo, Japan) operating at 200 kV (Shamsi et al., 2017).

2.2.7. Molecular docking analysis

Bioinformatics tools AutoDock 4 (Trott & Olson, 2010), Discovery studio (Biovia, 2015) and PyMOL (Schrodinger, 2010) were used for docking and visualization purposes. The 3-D coordinates of BSA and Al were retrieved from online resources such as Protein Data Bank (PDB) and PubChem.

Pre-processing of receptor and ligand: Atomic coordinates of BSA crystal structure and Al ligand were taken from the Protein Data Bank with PDB IDs: 4F5S and AL, respectively. The protein structure was subsequently preprocessed in SPDBV (Guex & Peitsch, 1997) and AutoDock Tools (Morris et al., 2009) followed by removing co-crystal ligands present in its coordinates file. Depending on the binding affinity and scoring, possible six top binding poses of Al with BSA were pooled out.

3. Results and discussion

3.1. Intrinsic fluorescence: Tertiary structure analysis

The conformational changes in the overall globular structure of protein were determined by measuring tryptophan fluorescence. BSA under native condition showed a peak at around 350 nm, which was due to intact tryptophan amino acid of the protein. As the time of incubation increases from 0 to 5 h at 65 °C, quenching was observed accompanied with blue shift of 9 nm (Fig. 1, inset). This observation supports the fact that at high temperature (65 °C), BSA undergoes various conformational changes and become more hydrophobic during unfolding pathway. One may also assume that the observed blue shift of λmax for BSA is due

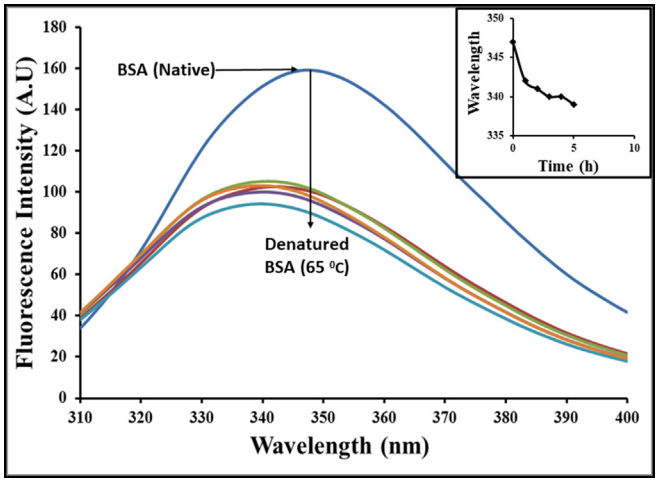

Fig. 1. Intrinsic fluorescence measurement: Fluorescence emission spectra of BSA incubated at 65 °C for different time interval at 0–5 h. Protein concentration used was 4 μM and was excited at 295 nm and emission intensity were recorded in between 300 and 400 nm. A graph was plotted between wavelength maxima Vs time of incubation of protein at 65 °C (Inset).

to transfer of Trp residues into more hydrophobic surroundings induced by dimerization of unfolded monomers (Borzova et al., 2016). A blue shift of the emission spectrum for tryptophan fluorescence observed for thermal unfolding of pig pancreas α-amylase (Duy and Fitter, 2006) and myosin subfragment1 (Markov et al., 2010) has been reported in the literature.

3.2. Extrinsic fluorescence: Hydrophobicity measurement

To study the interaction of BSA with ANS, we used the excitation wavelength of 380 nm (Wen et al., 2015). Under our study condition, fluorescence of ANS (alone) was found to be negligible (data not shown), however it was found to be markedly increased in the presence of intact BSA, suggesting the presence of numerous ANS binding sites in the protein molecule (Fig. 2). Further, at 65 °C, ANS binding with BSA was found to be decreased with increased incubation time as shown by quenching of fluorescence. Our observation is supported by well-known facts that incubation of protein at high temperature disrupts its hydrophobic patches. A similar result was also observed by chemical denaturants like urea and GdnHCl, which unfold proteins and quenches ANS fluorescence (Zhang et al., 2013). Our study further reaffirms the previous hypothesis that on thermal denaturation, the hydrophobic patches of BSA monomer gets exposed and are attracted to another monomer unit. This result in less hydrophobic residues are left to bind with ANS dye resulted in quenching of fluorescence.

3.3. Far UV-CD spectra: secondary structure analysis

To investigate the consequence of high temperature on the secondary structure of BSA, far UV-CD spectroscopy was performed (Fig. 3). BSA under native states (0 h), showed negative minima at around 208 nm and 222 nm wavelength. These negative peaks correspond to the α-helical structure of protein (Gelamo et al., 2002). With further increase of thermal stress (1 and 2 h of incubation), CD ellipticity was found to be decreased, suggesting a loss of α-helical structure and its conversion to other secondary structures (β-sheet and turn). After 5 h of incubation, the intensity of negative peak at 208 nm was found to be disappeared and a negative peak with high intensity at 222 nm appeared, which advocates the changes in the secondary structure of BSA incubated at 65 °C. The CD spectroscopic data indicate the transition of α-helical structure to other secondary forms like β-sheet and turn. Our observation is well supported by previous studies that illustrate 12 h preheating at 60 °C leading to a noticeable decrease by 22–37% in the α-helices portion and an increase in the portion of β-strands by 27–60%, and the portion of turns by 13–25% (Borzova et al., 2016). Other literature data show that heating of BSA to 65 °C at a constant rate (Gayen et al., 2008) or incubation at 90 °C for 10 min leads to a decrease in the portion of α-helices (Pearce et al., 2007).

3.4. Kinetics of aggregation by ThT assay

Thermal denaturation of BSA at 65 °C was further accessed to monitor amyloid formation using thioflavin (ThT) dye. This dye is specific for detection of amyloid observed in neurological diseases. It is generally accepted that the significant increase in ThT fluorescence is indicative of formation of amyloid fibrils, and are characterized by a cross-β-sheet rich structure (Borzova et al., 2016). Fig. 4 shows the ThT binding of BSA incubated at 65 °C at different time intervals. The results shows the rise in ThT fluorescence

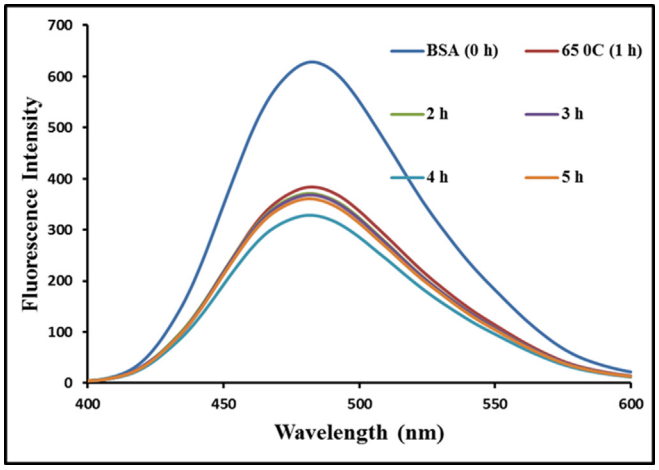

Fig. 2. ANS dye binding assay: The extrinsic ANS emission spectra showing exposure of hydrophobic patches of BSA incubated for 0–5 h at 65 °C. 50 M excess of ANS was added and fluorescence were recorded in between 400 and 600 nm after excitation at 380 nm.

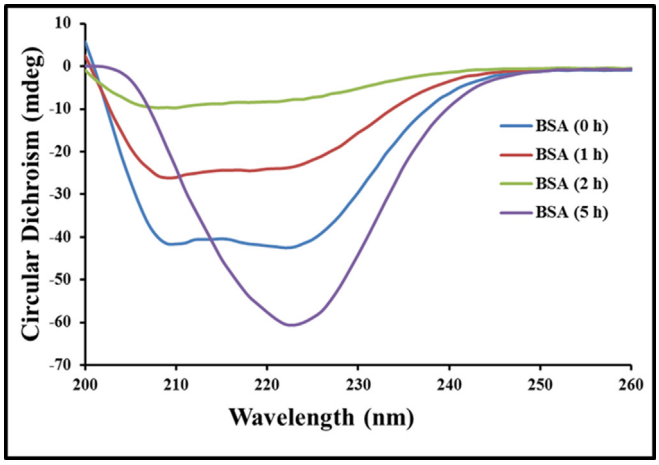

Fig. 3. Secondary structure analysis: Far UV-CD analysis of thermal denatured BSA at different time interval (0–5 h). It was scanned in between 190 and 260 nm. The reported spectrum is the average of three independent scan. Protein concentration was 0.2 mg/ml.

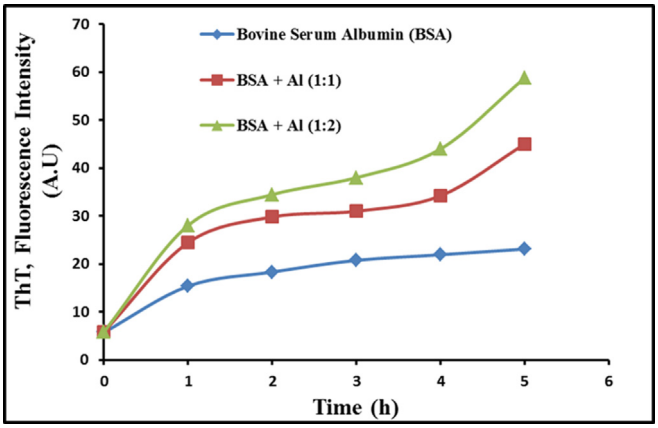

Fig. 4. Kinetics of thermal unfolding of BSA: Relative ThT fluorescence of BSA alone and with two different combination of Al (1:1 & 1:2). Maximum fluorescence intensity of ThT at 482 nm was plotted against different time interval.

intensity with increasing incubation time. This result is comparable to the results observed with hen egg white lysosome, amyloid beta and human islet amyloid polypeptide (Ghosh et al., 2015; Domanov & Kinnunen, 2008; Levine, 1993).

The effect of aluminium metal ion was also investigated on the kinetics of BSA aggregation incubated at 65 °C for 0–5 h. Aluminum was pre-incubated with BSA at 65 °C, for different time interval in the ratio of 1:1 and 1:2. ThT fluorescence was measured to explore the synergistic role of aluminum ion and temperature on the conformation of BSA. The results show that aluminum aggravates the conformational alteration of BSA (Fig. 4). The presence of aluminum and increased time of incubation show combinatorial effect resulting into enhancement of ThT fluorescence. At 1: 1 ratio of BSA to Al (III), 3-fold increase in ThT fluorescence was observed, while 6-fold increase recorded after 5 h incubation at 1:2 ratio. The concentration effect of aluminum on the kinetics of aggregation, suggests more distortion in the conformation of BSA by Al (III) leading to its fibrillation. Al (III) has been reported to accelerate the process of hIAPP fibril nucleation and aggregation (Xu, et al., 2016). In addition, Cu (II) has been shown to abrogate the process of fibrillation in thermal denatured human serum albumin (Panday et al., 2010). Moreover, other studies displaying Al(III)-induced fibrillation and aggregation involve the octahedral Al-O and Al-N bonding between aluminum and amyloidogenic proteins, forming O(N)-Al(III)-O(N) cross-links between protein monomers and leading to the amyloid nucleation and aggregation of protein (Yao et al., 2014; Ziang et al., 2012). Our finding is well supported by above-mentioned results.

3.5. Transmission electron microscopy (TEM) analysis

To determine the nature of aggregated structures and further confirming the presence of amyloid, TEM analysis was carried out. Fig. 5a (native BSA) showed normal protein structure without

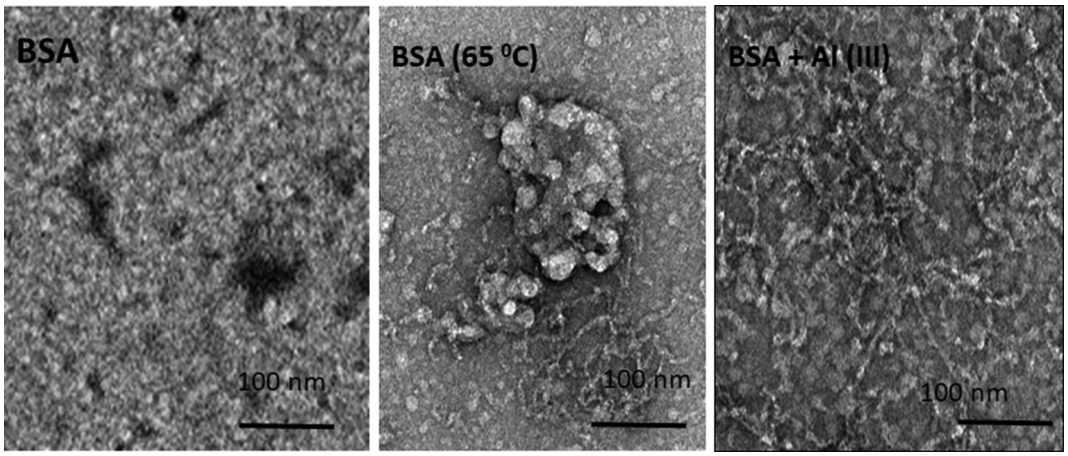

Fig. 5. Morphological (TEM) analysis: Transmission electron microscopy was performed to visualize pattern of protein aggregate and amyloid. (a) Control BSA, (B) Denatured BSA at 65 °C for 5 h, (C) Aluminium treated BSA.

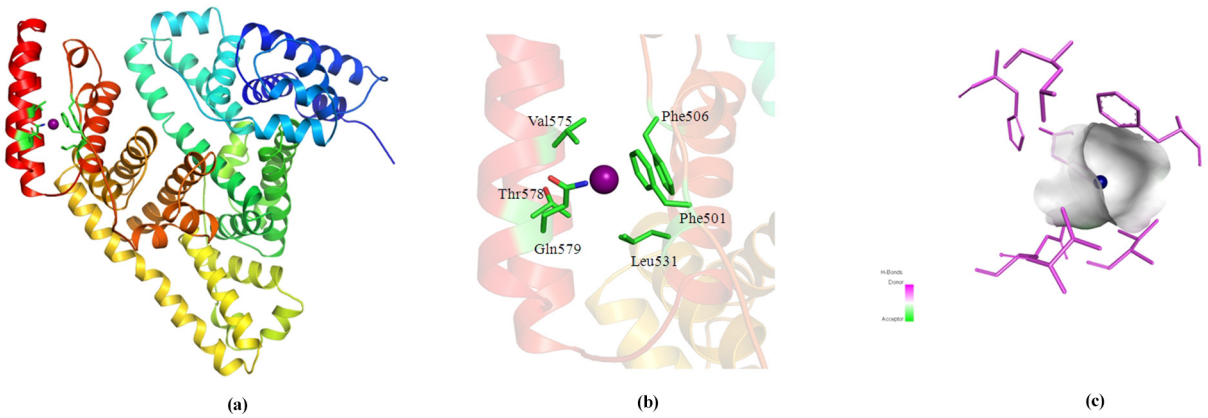

Fig. 6. Molecular docking analysis of Al metal ion with BSA protein. (a) conformation of the Al with BSA, (b) Interactions between BSA with Al, (c) residues playing a central role in Al-BSA interaction.

any aggregate. Fig. 5b and 5c illustrated BSA incubated for 5 h at 65 °C and BSA along with Al (III). From the results of TEM, one can hypothesize that thermal denaturation alone causes the formation of BSA aggregates and the addition of aluminum metal ions to BSA triggered intense fibril formation. Metal induced aggregate and amyloid formation has been reported earlier too (Tamás et al., 2014). Besides that, Cu (II) and Al (III) have also been reported to accelerate amyloid formation in protein (Xu, et al., 2016; Panday et al., 2010).

3.6. Molecular docking analysis

We observed several close interactions of Al towards important residues of BSA with significant binding affinity of −1.2 kcal/mol. The selected bound conformation of the Al with BSA has been shown in Fig. 6a. Several noteworthy interactions offered by the encompassing residues of BSA to Al are shown in Fig. 6b. The residues playing a central role in Al-BSA interaction were Phe501, Phe506, Val575, Thr578, Gln579, and Leu531 (Fig. 6b). Fig. 6c depicts Al in the vicinity of BSA. Thus, molecular docking advocated strong binding of Al and BSA that supports all our biophysical experiments.

4. Conclusion

In this study, BSA is used as a model protein to understand the underlying steps involved in aggregation process. The effect of aluminum metal ion on the process of thermal aggregation of BSA was also studied. Humans are largely exposed by aluminum due to their abundance in processed foods and contaminated drinking water. Aluminum can cross the blood- brain barrier along with carrier protein, deposits in the central nervous system and can play a crucial role in neurodegenerative diseases. Our study confirms the role of aluminum in the aggregation of BSA. We believe that our study will be helpful in drug designing against various neurodegenerative diseases.

Acknowledgment

The authors extend their appreciation to the Deanship of Scientific Research at KSU for funding this work through research group project number RGP-215.

References

Agnihotri, S.K., Kesari, K.K., 2019. Mechanistic Effect of Heavy Metals in Neurological Disorder and Brain Cancer. Networking of Mutagens in Environmental Toxicology. Springer, pp. 25–47.
Ahmed, A., Shamsi, A., Bano, B., 2017. Characterizing harmful advanced glycation end-products (AGEs) and ribosylated aggregates of yellow mustard seed phytocystatin: Effects of different monosaccharides. Spectrochim. Acta Part A Mol. Biomol. Spectrosc. 171, 183–192.
Biancalana, M., Koide, S., 2010. Molecular mechanism of Thioflavin-T binding to amyloid fibrils. Biochimica et Biophysica Acta (BBA)-Proteins and Proteomics 1804(7), 1405-1412.
Biovia, D.S., 2015. Materials Studio Modeling Environment. Dassault Systèmes, San Diego.
Bondy, S.C., 2014. Prolonged exposure to low levels of aluminum leads to changes associated with brain aging and neurodegeneration. Toxicology 315, 1–7.
Bondy, S.C., 2016. Low levels of aluminum can lead to behavioral and morphological changes associated with Alzheimer's disease and age-related neurodegeneration. Neurotoxicology 52, 222–229.
Borzova, V.A., Markossian, K.A., Chebotareva, N.A., Kleymenov, S.Y., Poliansky, N.B., Muranov, K.O., Stein-Margolina, V.A., Shubin, V.V., Markov, D.I., Kurganov, B.I., 2016. Kinetics of Thermal Denaturation and Aggregation of Bovine Serum Albumin. PLoS One. 11, (4) e0153495.
Domanov, Y.A., Kinnunen, P.K., 2008. Islet amyloid polypeptide forms rigid lipid–protein amyloid fibrils on supported phospholipid bilayers. J. Mol. Biol. 376 (1), 42–54.
Duy, C., Fitter, J., 2006. How aggregation and conformational scrambling fun folded states govern fluorescence emission spectra. Biophys. J. 90, 3704–3711.
Gayen, A., Chatterjee, C., Mukhopadhyay, C., 2008. GM1-induced structural changes of bovine serum albumin after chemical and thermal disruption of the secondary structure: a spectroscopic comparison. Biomacromolecules 9, 974–983.
Gelamo, E.L., Silva, C.H., Imasato, H., Tabak, M., 2002. Interaction of bovine (BSA) and human (HSA) serum albumins with ionic surfactants: spectroscopy and modelling. Biochim. Biophys. Acta 1594, 84–99.
Ghosh, S., Pandey, N.K., Banerjee, P., Chaudhury, K., Nagy., N.V., Dasgupta., S., 2015. Copper (II) directs formation of toxic amorphous aggregates resulting in inhibition of hen egg white lysozyme fibrillation under alkaline salt-mediated conditions. J. Biomol. Struct. Dynam., vol. 33, 5, pp. 991–1007.
Guex, N., Peitsch, M., 1997. CSWISS-MODEL and the Swiss-Pdb Viewer: an environment for comparative protein modeling. Electrophoresis 18 (15), 2714–2723.
Hedberg, Y.S., Pettersson, M.S., Pradhan, I., Wallinder, Odnevall, Rutland, M.W., Person, C., 2015. Can cobalt (II) and chromium (III) ions released from joint prostheses influence the friction coefficient? ACS Biomater. Sci. Eng. 1 (8), 617–620.
Huang, Q., Zhao, Q., Peng, J., Yu, Y., Wang, C., Zou, Y., Su, Y., Zhu, L., Wang, C., Yang, Y., 2019. Peptide-polyphenol (KLVFF/EGCG) binary modulators for inhibiting aggregation and neurotoxicity of amyloid-β peptide. ACS Omega 4 (2), 4233–4242.
Huat, T.J., Camats-Perna, J., Newcombe, E.A., Valmas, N., Kitazawa, M., Medeiros, R., 2019. Metal toxicity links to Alzheimer's disease and neuroinflammation. J. Mol. Biol. 431 (9), 1843–1868.
Islam, B., Jabir, N.R., Tabrez, S., 2019. The role of mitochondrial defects and oxidative stress in Alzheimer's disease. J. Drug Target. 27 (9), 932–942.
Jabir, N.R., Khan, F.R., Tabrez, S., 2018. Cholinesterase targeting by polyphenols: A therapeutic approach for the treatment of Alzheimer's disease. CNS Neurosci. Ther. 24, 753–762.
Khan, M.S., Bhat, S.A., Tabrez, S., Rehman, M.T., Al-okail, M., Alajmi, M.F., 2020. Quinoline yellow (Food additive) induced conformational changes in Lysozyme: A spectroscopic, docking and simulation studies of dye-protein interactions. Prep. Biochem. Biotech. https://doi.org/10.1080/10826068.2020.1725774.
Khan, M.S., Rabbani, N., Tabrez, S., Islam, B., Malik, A., Ahmed, A., Alsenaidy, M.A., Alsenaidy, A.M., 2016. Glycation induced generation of amyloid fibril structures by glucose metabolites. Protein Pept. Lett. 23 (10), 892–897.
Khan, M.S., Tabrez, S., Priyadarshini, M., Priyamvada, S., Khan, M.M.R., 2012. Targeting Parkinson's- tyrosine hydroxylase and oxidative stress as points of interventions. CNS & Neurol. Disorders - Drug Targets 11 (4), 369–380.
Schrodinger, L., 2010. The PyMOL molecular graphics system, Version 1(5).
Levine III, H., 1993. Thioflavine T interaction with synthetic Alzheimer's disease β-amyloid peptides: Detection of amyloid aggregation in solution. Protein Sci. 2 (3), 404–410.
Maczurek, A., Hager, K., Kenklies, M., Sharman, M., Martins, et al., 2008. Lipoic acid as an anti-inflammatory and neuroprotective treatment for Alzheimer's disease. Adv. Drug Deliv. Rev., vol. 60, 13-14, pp. 1463-1470.
Markov, D.I., Zubov, E.O., Nikolaeva, O.P., Kurganov, B.I., Levitsky, D.I., 2010. Thermal denaturation and aggregation of myosin sub fragment1isoforms with different essential light chains. Int. J. Mol. Sci. 11, 4194–4226.
Mezzaroba, L., Alfieri, D.F., Simão, A.N.C., Reiche, E.M.V., 2019. The role of zinc, copper, manganese and iron in neurodegenerative diseases. Neurotoxicology 74, 230–241.
Mishra, L., Sawant, P.D., Sundararajan, M.T., Bandyopadhyay, T., 2019. Binding of Cm (III) and Th (IV) with Human Transferrin at Serum pH: Combined QM and MD Investigations. J. Phys. Chem. B 123 (13), 2729–2744.
Mitra, G., 2019. Application of native mass spectrometry in studying intrinsically disordered proteins: A special focus on neurodegenerative diseases. Biochim. Biophys. Acta (BBA)-Prot. Proteom. 1867, 140260.
Morris, G.M., Huey, R., Lindstrom, W., et al., 2009. AutoDock4 and AutoDockTools4: Automated docking with selective receptor flexibility. J. Comput. Chem. 30 (16), 2785–2791.
Nusrat, S., Siddiqi, M.K., Zaman, M., Zaidi, N., Ajmal, M.R., Alam, P., Qadeer, A., Abdelhameed, A.S., Khan, R.H., 2016. A Comprehensive Spectroscopic and Computational Investigation to Probe the Interaction of Antineoplastic Drug Nordihydroguaiaretic Acid with Serum Albumins. PloS One 11, (7) e0158833.
Obrenovich, M., Tabrez, S., Siddiqui, B., McCloskey, B., Perry, G., 2020. The Microbiota-Gut-Brain Axis-Heart Shunt Part II Prosaic foods, The Brain-Heart Connection in Alzheimer disease. Microorganism 8, 493.
Ott, D.B., Hartwig, A., Stillman, M.J., 2019. Competition between Al 3+ and Fe 3+ binding to human transferrin and toxicological implications: structural investigations using ultra-high resolution ESI MS and CD spectroscopy. Metallomics 11 (5), 968–981.
Pandey, N.K., Ghosh, S., Dasgupta, S., 2010. Fibrillation in Human Serum Albumin Is Enhanced in the Presence of Copper(II). J. Phys. Chem. B 114, 10228–10233.
Pearce, F.G., Mackintosh, S.H., Gerrard, J.A., 2007. Formation of amyloid-like fibrils by ovalbumin and related proteins under conditions relevant to food processing. J. Agric. Food Chem. 55, 318–322.
Priest, N., Talbot, R., Newton, D., Day, J., King, S., Fifield, L., 1998. Uptake by man of aluminium in a public water supply. Hum. Exp. Toxicol. 17 (6), 296–301.
Sacchettini, J.C., Kelly, J.W., 2002. Therapeutic strategies for human amyloid diseases. Nat. Rev. Drug Discov. 1 (4), 267.
Shamsi, A., Ahmed, A., Bano, B., 2017. Structural transition of kidney cystatin induced by silicon dioxide nanoparticles: An implication for renal diseases. International Journal of Biological Macromolecules, 94, 754-761.

Tamás, M., Sharma, S., Ibstedt, S., Jacobson, T., Christen, P., 2014. Heavy metals and metalloids as a cause for protein misfolding and aggregation. Biomolecules 4 (1), 252–267.

Taylor, J.P., Hardy, J., Fischbeck, K.H., 2002. Toxic proteins in neurodegenerative disease. Science 296 (5575), 1991–1995.

Trott, O., Olson, A.J., 2010. AutoDock Vina: improving the speed and accuracy of docking with a new scoring function, efficient optimization, and multithreading. J. Comput. Chem. 31 (2), 455–461.

Vaquer-Alicea, J., Diamond, M.I., 2019. Propagation of protein aggregation in neurodegenerative diseases. Annu. Rev. Biochem. 88, 785–810.

Wen, L., Chen, Y., Liao, J., Zheng, X., Yin, Z., 2015. Preferential interactions between protein and arginine: effects of arginine on tertiary conformational and colloidal stability of protein solution. Int. J. Pharm. 478, 753–761.

Xu, Z.-X., Zhang, Q., Ma, G.-L., et al., 2016. Influence of aluminium and EGCG on fibrillation and aggregation of human islet amyloid polypeptide. J. Diab. Res. https://doi.org/10.1155/2016/1867059. Article ID 1867059.

Xue, C., Lin, T.Y., Chang, D., Guo, Z., 2017. Thioflavin T as an amyloid dye: fibril quantification, optimal concentration and effect on aggregation. R Soc Open Sci. 4, (1) 160696.

Yao, T., Jiang, T., Pan, D., Xu, Z.-X., Zhou, P., 2014. Effect of Al(III) and curcumin on silk fibroin conformation and aggregation morphology. RSC Adv. 4 (76), 40273–40280.

Yokel, R.A., Rhineheimer, S.S., Sharma, P., Elmore, D., McNamara, P.J., 2001. Entry, half-life, and desferrioxamine-accelerated clearance of brain aluminum after a single 26Al exposure. Toxicol. Sci. 64 (1), 77–82.

Zhang, C., Gao, C., Mu, J., Qiu, Z., Li, L., 2013. Spectroscopic Studies on Unfolding Processes of Apo-Neuroglobin Induced by Guanidine Hydrochloride and Urea. BioMed Research International, Article ID 349542, 1–7.